



MR. DONGHAI WU (Orcid ID : 0000-0002-4638-3743)

DR. SHILONG PIAO (Orcid ID : 0000-0001-8057-2292)

DR. XUHUI WANG (Orcid ID : 0000-0003-0818-9816)

Article type : Primary Research Articles

Article Type: Primary Research Articles

## Accelerated terrestrial ecosystem carbon turnover and its drivers

Running title: Changes of ecosystem carbon turnover time

Donghai Wu<sup>1</sup>, Shilong Piao<sup>1,2,3\*</sup>, Dan Zhu<sup>4</sup>, Xuhui Wang<sup>1</sup>, Philippe Ciais<sup>4</sup>, Ana Bastos<sup>5</sup>, Xiangtao Xu<sup>6</sup>, Wenfang Xu<sup>7</sup>

<sup>1</sup>Sino-French Institute for Earth System Science, College of Urban and Environmental Sciences, Peking University, Beijing 100871, China.

<sup>2</sup>Key Laboratory of Alpine Ecology, Institute of Tibetan Plateau Research, Chinese Academy of Sciences, Beijing 100085, China.

<sup>3</sup>Chinese Academy of Sciences Center for Excellence in Tibetan Plateau Earth Science, Chinese Academy of Sciences, Beijing 100085, China.

<sup>4</sup>Laboratoire des Sciences du Climat et de l'Environnement (LSCE), CEA CNRS UVSQ, Gif Sur Yvette 91191, France.

This article has been accepted for publication and undergone full peer review but has not been through the copyediting, typesetting, pagination and proofreading process, which may lead to differences between this version and the [Version of Record](#). Please cite this article as [doi: 10.1111/GCB.15224](#)

This article is protected by copyright. All rights reserved

---

<sup>5</sup>Department of Geography, Ludwig-Maximilians Universität, Luisenstr. 37, 80333, Munchen, Germany.

<sup>6</sup>Department of Ecology and Evolutionary Biology, Cornell University, Ithaca, NY 14853, USA.

<sup>7</sup>School of Atmospheric Sciences, Sun Yat-sen University, Zhuhai 519082, Guangdong, China.

\* Correspondence: Shilong Piao, Email: slpiao@pku.edu.cn

## Abstract

The terrestrial carbon cycle has been strongly influenced by human-induced CO<sub>2</sub> increase, climate change and land use change since the industrial revolution. These changes alter the carbon balance of ecosystems through changes in vegetation productivity and ecosystem carbon turnover time ( $\tau_{eco}$ ). Even though numerous studies have drawn an increasingly clear picture of global vegetation productivity changes, global changes in  $\tau_{eco}$  are still unknown. In this study, we analyzed the changes of  $\tau_{eco}$  between the 1860s and the 2000s and their drivers, based on theory of dynamic carbon cycle in non-steady state and process-based ecosystem model. Results indicate that  $\tau_{eco}$  has been reduced (i.e. carbon turnover has accelerated) by 13.5% from the 1860s (74 years) to the 2000s (64 years), with reductions of 1 year of carbon residence times in vegetation ( $r_{veg}$ ) and of 9 years in soil ( $r_{soil}$ ). Additionally, the acceleration of  $\tau_{eco}$  was examined at biome scale and grid scale. Among different driving processes, land use change and climate change were found to be the major drivers of turnover acceleration. These findings imply that carbon fixed by plant photosynthesis is being lost from ecosystems to the atmosphere more quickly over time, with important implications for the climate-carbon-cycle feedbacks.

**Keywords:** Carbon turnover time, ecosystem, vegetation, soil, CO<sub>2</sub> increase, climate change, land use change

---

## 1. Introduction

Ecosystem carbon turnover time ( $\tau_{eco}$ ) and net primary production (NPP) are the two dominant factors determining the magnitude and dynamics of ecosystem carbon storage (Koven et al., 2015).  $\tau_{eco}$  represents the mean time that carbon atoms reside in the ecosystem, from influx via NPP to outflux mainly via heterotrophic respiration and disturbances (e.g. fire) (Appendix S1 and Fig. S1). Ecosystem carbon turnover time is further controlled by other processes, including carbon allocation, plant organ mortality rates, and soil organic carbon decomposition rates (Xia, Luo, Wang, & Hararuk, 2013). Although the carbon turnover processes are complex, researchers usually estimate the  $\tau_{eco}$  indirectly as the ratio between the mass of ecosystem carbon storage and NPP (pool/flux) based on the assumption of steady state conditions (Lu, Wang, Luo, & Jiang, 2018; Zhou et al., 2018). Observation-based steady-state  $\tau_{eco}$  distributions have been used to assess the environmental drivers of spatial variability in  $\tau_{eco}$ , and used as a benchmark for ecosystem models (Carvalhais et al., 2014).

Human-induced CO<sub>2</sub> increase, climate change and land use change have profoundly altered the terrestrial ecosystem carbon dynamics since the 1860s (Piao et al., 2020; Fernández-Martínez et al., 2019; Liu et al., 2019; Piao et al., 2018; Sitch et al., 2015). On the one hand, global vegetation productivity shows an increasing trend from satellite greenness data and ecosystem models (Piao et al., 2020; Kolby Smith et al., 2016), mainly induced by CO<sub>2</sub> fertilization (Liu et al., 2019; Zhu et al., 2016), by extended phenology in response to warming (Peñuelas et al., 2017), and by afforestation and ecosystem conservation (Chen et al., 2019; Zhu et al., 2016). On the other hand, these driving factors also affected  $\tau_{eco}$  (Erb et al., 2016; Koven et al., 2015). For example, global warming could accelerate soil microbial decomposition, which results in shorter carbon residence time in the soil ( $r_{soil}$ ); forest to cropland conversion accelerates carbon residence time in the vegetation ( $r_{veg}$ ). Based on theory and experiments, CO<sub>2</sub> fertilization may also alter  $r_{veg}$  by changing carbon allocation and mortality rates (Brienen et al., 2015; Bugmann & Bigler, 2011; De Kauwe et al., 2014) and changing  $r_{soil}$  by reducing regional soil water loss through transpiration (Van Groenigen, Osenberg, & Hungate, 2011) due to increased water use efficiency by plants.

---

This implies that  $\tau_{eco}$  in the real world is dynamic. However, until now, changes of terrestrial  $\tau_{eco}$  and their specific drivers since industrial evolution have not been quantified yet.

Even though the approximation of pool/flux under steady-state can be applied for the static  $\tau_{eco}$  patterns, implicit error problems may arise if this assumption is used to evaluate the dynamics of non-steady-state carbon cycling systems. For example, such approximation could result in erroneous ecosystem  $\tau_{eco}$  values because of the “apparent change” phenomenon induced by lagged responses of carbon pools with slower cycling rates under the conditions of changes of carbon inputs caused by external environmental changes (Methods and Appendix S3) (Koven et al., 2015). Based on the dynamic carbon cycling theory (Luo et al., 2017; Rasmussen et al., 2016), dynamic  $\tau_{eco}$  can be computed by an invertible matrix of cycling and transfer rates (**A**), and a matrix of carbon allocation rates (**B**). For matrix **A**, ecosystem variables related to biomass pools mortality and litterfall rates, SOC pools decomposition rates and transfer rates between pools are needed. For matrix **B**, NPP allocation rates in biomass pools (fruit, leaf, root and wood) are required. In reality, not so many system variables can be observed globally to support the analysis of changes in  $\tau_{eco}$ . Therefore, an ecosystem process model can give insights about this emergent scientific question for  $\tau_{eco}$  changes and its driving factors.

In this study, ORCHIDEE-MICT was applied for studying the changes of ecosystem carbon turnover time. ORCHIDEE-MICT (Guimberteau et al., 2018; Zhu et al., 2016) is a recently developed ecosystem model, which has the advantage of discretizing soil carbon vertically and of considering processes influencing permafrost carbon in the high-latitude regions. To quantify temporal changes of ecosystem carbon turnover times and their environmental drivers (CO<sub>2</sub> increase, climate change and land use change), we performed six experimental simulations (S1-S6) using long-term forcing datasets after simulating an initial steady state spin-up run for carbon pools. Matrices **A** and **B** were established with all the pool and flux variables related with carbon turnover given by ORCHIDEE-MICT, and carbon turnover times were computed for different scenarios and at different spatial scales for two periods (the 1860s decade representing terrestrial ecosystems in the early stage of the industrial revolution, and the 2000s decade

---

representing terrestrial ecosystems in the present-day).

## 2. Materials and methods

### 2.1 ORCHIDEE-MICT model and simulations

ORCHIDEE-MICT is an improved ecosystem model (Guimberteau et al., 2018; Zhu et al., 2016) derived from the ORCHIDEE model (Krinner et al., 2005). The carbon cycle frameworks of the two models are similar, except for the soil pools which have been improved in ORCHIDEE-MICT through discretizing the soil profile into 32 layers with a total soil depth of 38m. Furthermore, ORCHIDEE-MICT has largely improved the performance of carbon cycle modeling in permafrost regions by incorporating processes such as SOM-dependent soil thermal and hydraulic parameters and optimizing parameters of soil thermal and hydraulic processes. In ORCHIDEE-MICT, there are five vegetation pools (fruit, leaf, reserve, root and wood), four litter pools (aboveground metabolic and structural litter pools, and belowground metabolic and structural litter pools), and three soil pools (active, slow and passive) in each soil layer (Fig. S2). Similar to the ORCHIDEE model, ORCHIDEE-MICT distinguishes 12 plant function types (PFTs, of which 10 are natural and two agricultural).

In this study, we performed six factorial simulations (S1-S6) using ORCHIDEE-MICT model to analyze the changes of carbon turnover times. Three long term forcing datasets (changing CO<sub>2</sub>, climate and land use) from 1860 to 2016 were used to run the model. Global atmospheric CO<sub>2</sub> forcing were constructed by station observations (MLO and SPO) provided by NOAA's Earth System Research Laboratory (<http://www.esrl.noaa.gov/gmd/ccgg/trends/>) after 1958 and data inversion with a cubic spline fit to ice core data (Joos & Spahni, 2008) prior to 1958. A 6-hourly, 0.5°×0.5° CRU-NCEP climatic forcing dataset were used to represent the historical climate dynamics between 1901 and 2016, and years selected from the 1901-1920 period were used to fill the forcing for 1860-1900 (Wei et al., 2014). Land use forcing was implemented with latest HYDE land use/land cover change datasets (Goldewijk, 2001).

First, an initial steady state spin-up for carbon and water pools was run for preindustrial

---

conditions, applying fixed atmospheric CO<sub>2</sub> concentration, the 1901-1920 CRU-NCEP climate forcing in a loop, and land cover map at the 1860 level. Simulations S1-S5 started from this spin-up state.

In simulation S1, the model was forced by varying CO<sub>2</sub> only, with fixed climate (recycling 1901-1920 climate) and land cover (1860); simulation S2 was prescribed with historical CO<sub>2</sub> and climate, keeping land cover fixed (1860); in simulation S3, the closest to the real world, the model was prescribed with varying CO<sub>2</sub>, climate and land use change; simulation S4 was prescribed with varying climate only, keeping CO<sub>2</sub> and land-cover fixed (1860); in simulation S5, the model was prescribed with varying land use change only, keeping CO<sub>2</sub> and climate fixed (1860 for CO<sub>2</sub> and recycling spin up climate). Results of S1-S5 were used to identify the relative contribution of main driving factors on changes of carbon turnover times, representing CO<sub>2</sub> effect (S1), CO<sub>2</sub>+climate effects (S2), CO<sub>2</sub>+climate+land use change effects (S3), climate effect (S4) and land use change effect (S5) respectively.

As a major disturbance, fire plays an important role in carbon turnover processes, and may also affect changes in  $\tau_{eco}$ . We therefore conducted an additional simulation (S6) with ORCHIDEE-MICT with the fire module off (thus no fire-induced mortality and carbon emissions). Before the historical simulation, a new initial steady state spin-up without fire processes was run, under a similar setup as that used for S1-S5. Starting from the spin-up state, simulation S6 was prescribed with varying CO<sub>2</sub>, climate and land use change. Therefore, comparison between S6 (fire-off) and S3 (fire-on) can demonstrate the fire effects on  $\tau_{eco}$ .

In this study, variables were saved annually on a 1°×1° grid for each carbon pools in the ORCHIDEE-MICT model (five vegetation pools, four litter pools, and three soil pools at each layer), and related influx and outflux for each carbon pools (Fig. S2). All variables were used to establish the matrices **A** and **B**, which were used to study the dynamics of terrestrial ecosystem carbon turnover times. Here, we focused on two periods in the 1860s (1860-1869) and 2000s (2000-2009), representing terrestrial ecosystem in the early stage of the industrial revolution and in present day, to analyze the changes of carbon turnover times and their driving mechanisms.

---

## 2.2 Model evaluation

To assess the reliability of our results, we carefully evaluated the overall performance of ORCHIDEE-MICT compared to independent observation-based datasets in four aspects (Appendix S2): (1) ecosystem carbon storage, NPP and  $\tau_{eco}$  on global scale; (2) ecosystem carbon storage, NPP and  $\tau_{eco}$  on grid scale; (3) spatially climatic sensitivities of NPP and  $\tau_{eco}$ ; and (4) temporal CO<sub>2</sub> exchanges between the atmosphere and the terrestrial biosphere. Results indicated that ORCHIDEE-MICT captured well the static and dynamic patterns of these variables. Therefore, ORCHIDEE-MICT is an appropriate ecosystem model to study the temporal changes of carbon turnover.

## 2.3 Ecosystem carbon turnover time under dynamic system in non-steady state

Carbon cycle models can be expressed in matrix form based on the mass conservation principle (Anderson, 1983; Bolin, 1981; Luo, Keenan, & Smith, 2015). For a dynamic carbon cycling system in non-steady state with  $d$  carbon pools, the matrix form can usually be described as (Luo et al., 2017):

$$d\mathbf{X}(t)/dt = \dot{\mathbf{X}}(t) = \mathbf{A}(t) \cdot \mathbf{X}(t) + \mathbf{B}(t) \cdot \mathbf{U}(t) \quad (1)$$

Where  $\mathbf{X}(t) \in \mathbb{R}^{d \times 1}$  is the carbon storage for year  $t$  and  $\dot{\mathbf{X}}(t) \in \mathbb{R}^{d \times 1}$  represents the balance of carbon pools for year  $t$ .  $\mathbf{A}(t) \in \mathbb{R}^{d \times d}$  describes the cycling rates for each carbon pool and the transfer rates between carbon pools for year  $t$ .  $\mathbf{A}$  is an invertible matrix and  $\{a_{ij}\}_{i,j \in \{1,\dots,d\}}$  satisfy: (1) for all  $i \in \{1,\dots,d\}$ ,  $a_{ii} < 0$ ; (2) for all  $i \neq j \in \{1,\dots,d\}$ ,  $a_{ij} \geq 0$ ; (3) for all  $j \in \{1,\dots,d\}$ ,  $\sum_{i=1}^d a_{ij} \leq 0$ . The  $i$ -th row in  $\mathbf{A}$  represents the carbon dynamics of the  $i$ -th pool:  $a_{ij}$  is the transfer rate from pool  $j$  to pool  $i$ ;  $a_{ii}$  is the cycling rate of pool  $i$ , including transfer to other pools and losses from the system.  $\mathbf{B}(t) \in \mathbb{R}^{d \times 1}$  represents the carbon allocation fractions to the  $d$  pools for year  $t$ .  $\mathbf{U}(t) \in \mathbb{R}^{1 \times 1}$  is the total system influx. It should be noted that this is a general linear nonautonomous system representation for dynamic carbon cycle processes, and vectors in the matrix equation are time-dependent (Sierra, Ceballos-Núñez, Metzler, & Müller, 2018).

---

Furthermore, the matrix expression can be applied to the ecosystem, or separately for the vegetation or soil systems. In this study, we applied the matrix expression to the ecosystem.

The terrestrial carbon cycle is in non-steady state in response to the human induced CO<sub>2</sub> increase, climate change and land use change, and variables in the system show significant trends since the pre-industrial period. To describe the carbon turnover time of a dynamic system in non-steady state, equation (1) can be transformed into (Luo et al., 2017):

$$\mathbf{X}(t) - \mathbf{A}(t)^{-1} \cdot \dot{\mathbf{X}}(t) = -\mathbf{A}(t)^{-1} \cdot \mathbf{B}(t) \cdot \mathbf{U}(t) \quad (2)$$

Where  $\mathbf{X}(t) \in \mathbb{R}^{d \times 1}$  is the carbon storage for year  $t$ ,  $-\mathbf{A}(t)^{-1} \cdot \dot{\mathbf{X}}(t) \in \mathbb{R}^{d \times 1}$  is the storage potential based on system status for year  $t$  and  $-\mathbf{A}(t)^{-1} \cdot \mathbf{B}(t) \cdot \mathbf{U}(t) \in \mathbb{R}^{d \times 1}$  is the storage capacity based on the system state for year  $t$ . Here, the carbon capacity represents the maximum amount of carbon that an ecosystem can store at given environmental conditions for year  $t$ , which indicate the instantaneous responses of the land carbon cycle to external forcings (e.g. atmospheric CO<sub>2</sub> concentration, climate and land cover types (Luo et al., 2017). The ecosystem carbon storage potential was defined as the difference between the ecosystem carbon storage capacity and the current carbon storage ( $\mathbf{X}(t) \in \mathbb{R}^{d \times 1}$ ). Therefore, the ecosystems would act as a carbon sink when the carbon storage potential is positive, and a carbon source when carbon storage potential is negative. In addition, we can describe the mean carbon residence times in all carbon pools as (Luo et al., 2017):

$$\mathbf{R}(t) = -\mathbf{A}(t)^{-1} \cdot \mathbf{B}(t) \in \mathbb{R}^{d \times 1} \quad (3)$$

If we summate both sides of the equation for all pools (2), the formula can be rewritten as:

$$\sum(\mathbf{X}(t) - \mathbf{A}(t)^{-1} \cdot \dot{\mathbf{X}}(t)) = \sum \mathbf{R}(t) \cdot \mathbf{U}(t) \quad (4)$$

Therefore, the system carbon turnover time can be described as:

$$\tau(t) = \sum(\mathbf{X}(t) - \mathbf{A}(t)^{-1} \cdot \dot{\mathbf{X}}(t)) / \mathbf{U}(t) = \sum \mathbf{R}(t) = \sum(-\mathbf{A}(t)^{-1} \cdot \mathbf{B}(t)) \quad (5)$$

We conclude that the carbon turnover time ( $\tau(t)$ ), defined as the ratio between the storage capacity and carbon influx ( $\mathbf{U}(t)$ ), equals to the sum of the carbon residence times ( $\mathbf{R}(t)$ ).

---

Furthermore, the system carbon turnover time ( $\tau(t)$ ) is closely related to the variables in matrix  $\mathbf{A}(t)$  and  $\mathbf{B}(t)$ . Therefore, it is clear that traditional methods for directly calculating the carbon turnover time with  $\sum \mathbf{X}(\mathbf{t})/\mathbf{U}(\mathbf{t})$  must satisfy the steady state assumption ( $\dot{\mathbf{X}}(t) \approx 0$ ). It is, thus, not reasonable to apply the method of  $\sum \mathbf{X}(\mathbf{t})/\mathbf{U}(\mathbf{t})$  in a dynamic system in non-steady state. In this work, we treat the ecosystem, including vegetation and soil (including litter pools), as an integrated system. Ecosystem turnover time ( $\tau_{eco}$ ) equals to the sum of the carbon residence time in vegetation ( $r_{veg}$ ) and in soil ( $r_{soil}$ , including litter pools) pools (Appendix S1).

#### 2.4 “Apparent change” phenomenon induced by pool/flux approach in non-steady state

The “apparent change” occurs when we compute the system carbon turnover times using pool/flux approach in non-steady state. We carefully elaborated the mechanisms behind this phenomenon with a case model in Appendix S3. In general, “apparent change” is induced by lagged responses of ecosystem carbon pools with slower cycling rates (e.g. slow pool and passive pool) due to changes in carbon inputs caused by external environmental changes (e.g. CO<sub>2</sub> increase, global warming and land use change). The “apparent change” could therefore mislead the estimate of changes of carbon turnover times and their driving mechanisms.

Based on output variables from ORCHIDEE-MICT, we further tested the theory of dynamic carbon cycle in non-steady state (Appendix S4). We computed the carbon turnover times with two methods: (1)  $\sum \mathbf{X}(\mathbf{t})/\mathbf{U}(\mathbf{t})$  (i.e. Ceco/NPP) from the steady state assumption; and (2)  $\sum (-\mathbf{A}(t)^{-1} \cdot \mathbf{B}(t))$  based on dynamic theory. The results suggested that the carbon cycle in the 2000s is in non-steady state, and that the calculation of global  $\tau_{eco}$  with Ceco/NPP results in the underestimation of the intrinsic value in non-steady state by 8% for ORCHIDEE-MICT (Fig. S10). Therefore, we recommend choosing the matrix inversion method to study the changes of  $\tau_{eco}$  and their drivers to avoid potential issues caused by the “apparent change”.

### 3. Results

#### 3.1 Changes of ecosystem carbon turnover time

Our simulation showed that the global ecosystem carbon turnover time ( $\tau_{eco}$ ) has been

---

reduced, i.e. turnover has accelerated over time, by 13.5% from the 1860s ( $\tau_{eco} = 74$  years) to the 2000s ( $\tau_{eco} = 64$  years) (Fig. 1). Among the different driving processes evaluated, land use change played the strongest role, leading to a reduction of  $\tau_{eco}$  of 5.9 years, followed by climate change (reduction of 3.5 years). A negative effect on turnover time is also found for CO<sub>2</sub> increase, but the magnitude is smaller compared to the preceding two processes (0.8 year). When separating  $\tau_{eco}$  into carbon residence times in vegetation ( $r_{veg}$ ) and in soil ( $r_{soil}$ ), the effects of driving factors are quite different.  $r_{veg}$  has been reduced by 9.4% (1 year) from the 1860s and the 2000s, with a trade-off between strong negative effects from land use change and smaller positive effects from increasing CO<sub>2</sub> (Fig. 1d). According to the model, climate change did not have a significant effect on  $r_{veg}$  at the global scale. By contrast,  $r_{soil}$  was reduced by 14.1% (9 years), with similar driving factors to those of  $\tau_{eco}$  (Fig. 1e, f).

We found different reductions of  $\tau_{eco}$  across different biomes from the 1860s to the 2000s and different driving processes (Fig. 2 and Fig. S12). Boreal forests have the smallest relative reduction of  $\tau_{eco}$  (-4%), while cropland experienced the fastest acceleration (-25%) in this period. The land use change is the main factor behind differences between biomes, having very small effects on  $\tau_{eco}$  in boreal forest, and the largest effects in cropland (-9.3 years). Climate change generally had significant negative effects on  $\tau_{eco}$ , with the largest influence in grassland and the smallest influence in tropical forest (Fig. S12). By contrast, increasing CO<sub>2</sub> did not significantly affect  $\tau_{eco}$  across most biomes except for a small positive effect in tropical forests. The effects of each driving factor on  $r_{soil}$  were similar to those on  $\tau_{eco}$ , while the response of  $r_{veg}$  has different sign and magnitude to increasing CO<sub>2</sub> and climate change. Increasing CO<sub>2</sub> has positive effects on  $r_{veg}$  across all biomes. Thus, the overall non-significant effect of increasing CO<sub>2</sub> on  $\tau_{eco}$  could be explained by the trade-off between a negative effect (acceleration) on  $r_{soil}$  and a positive effect (slow-down) on  $r_{veg}$ . Climate change had negative effects on  $r_{veg}$  in grassland and cropland, but positive effects in tropical forests and boreal forests. Nevertheless, the magnitude of climate change effects on  $r_{veg}$  is small, compared to other driving factors.

Finally, we analyzed the spatial patterns of changes of  $\tau_{eco}$  at the grid scale (Fig. 3, Fig. S13

and Fig. S14).  $\tau_{eco}$  has accelerated in most parts of the globe (~83% of vegetated area), with the largest acceleration found in agricultural regions (eastern America, eastern China, India and sub-Saharan), grassland dominated regions (southeast South America, southern Africa and eastern Australia), and tropical forests (Indonesia), and relative smaller acceleration in boreal regions (northern North America and Siberia). The largest acceleration values were mainly associated with regional land use change, consistent with the biome-scale results. The spatial patterns of the acceleration of  $r_{soil}$  are similar with those of  $\tau_{eco}$ , while  $r_{veg}$  has different patterns.  $r_{veg}$  has increased in most boreal regions, and also in some temperate regions (northeast America, Europe and China). In most boreal regions, the dominant driving factors are climate change and increasing CO<sub>2</sub>. By contrast, increasing  $\tau_{veg}$  in temperate regions was mainly explained by regional land use change. In general,  $\tau_{eco}$  over 44% of the global vegetated area has been reduced by land use change, over 33% by climate change, and over 6% by increasing CO<sub>2</sub>.

### 3.2 Fire effects on ecosystem carbon turnover time

We calculated the effects of fire in  $\tau_{eco}$  based on fire-on and fire-off simulations. Results suggest that fire mainly affects  $\tau_{eco}$  in boreal forests and in African grasslands (Fig. S15), consistent with the higher fire occurrence in these regions (Giglio, Randerson, & Werf, 2013). For example, fire shortens the  $\tau_{eco}$  by more than 20% in the sub-Saharan regions. Then, we calculated the changes of  $\tau_{eco}$  between 1860s and 2000s based on fire-on and fire-off simulations. We found no significant differences of the relative changes of  $\tau_{eco}$  on either global scale (Fig. S16) or on grid scale (Fig. S17) possibly because the simulations do not account for human driven historical fire changes (Knorr, Arneth, & Jiang, 2016; Mouillet & Field, 2005). Therefore, although fire plays significant effect on the patterns of  $\tau_{eco}$ , fire effect on the trend of  $\tau_{eco}$  is weak in our simulations.

### 3.3 Ecosystem carbon storage change and potential

Accelerated  $\tau_{eco}$  implied that carbon atoms fixed by plant photosynthesis stay shorter time in terrestrial ecosystems in the 2000s, compared to early stage of the industrial revolution. In parallel, global ecosystem productivity has increased during this period ( $41 \pm 1$  Pg C yr<sup>-1</sup> in 1860s vs.  $53 \pm 1$

---

Pg C yr<sup>-1</sup> in 2000s). These combined processes resulted in an ecosystem carbon sink from the 1860s to the 2000s in most regions, especially in the tropics and high latitudes (Fig. 4a and Fig. S18), which played a significant role in mitigating the human-induced carbon emissions into atmosphere (Ciais et al., 2014). According to ORCHIDEE-MICT, both vegetation and soils have contributed to the carbon sink (Fig. 4c, e and Fig. S18), which is supported by observation-based studies (Pan et al., 2011).

Beyond the historical change, we are interested in whether the present-day terrestrial ecosystems in non-steady state have extra potential for carbon sequestration. Here, the ecosystem carbon storage potential was defined as the difference between the ecosystem carbon storage capacity and the present-day carbon storage (Methods). Results from the analysis of the ecosystem carbon storage potential indicated as carbon sink in high northern latitudes and in some temperate forests (northeast America, Europe and China), but a saturation of the carbon sink or even a carbon source elsewhere (Fig. 4 and Fig. S18). It should however be noted that in the model the carbon sink function in tropical forest biomass tends to saturation. To sum up, terrestrial ecosystems could storage carbon up to 763 Pg based on the current system state, with 41 Pg C in vegetation and 722 Pg C in soil. Noticeably, China accounted for 25% global vegetation carbon potential, mainly in the afforested regions.

#### 4. Discussion

##### 4.1 Impacts from land use change

It is remarkable that human-induced land use change has such a strong effect on  $\tau_{eco}$ , however, our results indicate both positive (slow-down) and negative (acceleration) impacts. The negative effects of land use change on  $\tau_{eco}$  occurred in most parts of world, mainly because of cropland expansion at the expense of the natural forests and grasslands (Fig. S19 and Fig. S20) (Foley et al., 2005; Ramankutty & Foley, 1999). In contrast, positive effects of land use change on  $\tau_{eco}$  are found in some temperate regions with increasing forest cover, and conversion from agricultural to natural vegetation. The enhanced forest fraction can be attributed to afforestation in China (Chen et al., 2019) and forest conservation in Europe (Luyssaert et al., 2010; McGrath et al.,

---

2015). A related study also concluded that land use change greatly reduced biomass turnover times globally (Erb et al., 2016). Nevertheless, it should be noted that the change of biomass turnover times in previous study compared present-day ecosystem state under the assumption on steady-state and a hypothetical condition in the absence of land use but under current climate (Erb et al., 2016). By contrast, our study makes a step forward to decomposing the effects of CO<sub>2</sub> increasing, climate change and land use change based on a dynamic system rather than a steady-state one.

Furthermore, only net land cover transitions were accounted for the land use change processes simulated by ORCHIDEE-MICT, and that the simultaneous, bidirectional transitions between two vegetation types within the same grid cell were not considered (Arneth et al., 2017; Yue et al., 2018). Even though the conclusions of this study would not be affected by these processes, considering the bidirectional transitions in the model could provide a clearer picture for the effects of land use change on  $\tau_{eco}$  changes, especially on shorter time scales (e.g. decades). The effects from bidirectional transitions should be specially explored in future work.

#### 4.2 Changes of vegetation carbon residence time

The mechanisms behind changes in  $\tau_{eco}$  for vegetation and soil components can be explained by the specific processes in each pool.  $r_{veg}$  is mainly dominated by the residence time in woody pools which can be estimated as the ratio between the wood allocation proportion ( $all_w$ ) and the wood turnover rates ( $k_w$ ) including senescence, mortality and external disturbances (e.g. fire) (Thurner et al., 2016). This robust relationship is well simulated by ORCHIDEE-MICT (Fig. S21). Thus, we can further explain the changes of  $r_{veg}$  via examining the response patterns of  $all_w$  and  $k_w$  to the environmental drivers (Fig. S22). At the global scale, increasing CO<sub>2</sub> increased  $all_w$  (+5%) and decreased  $k_w$  (-3%), resulting in positive effects of CO<sub>2</sub> on  $r_{veg}$ . In contrast, land use change has significantly decreased  $all_w$  (-2%) and increased  $k_w$  (+18%), which led to shorter  $r_{veg}$ . Lengthened  $r_{veg}$  due to increasing  $all_w$  (2%) by climate change has been partly offset by increasing  $k_w$  (1%). Because effects of land use change are stronger than those of increasing CO<sub>2</sub>,  $r_{veg}$  ultimately accelerated. The sign and magnitude of  $all_w$  and  $k_w$  in responses to the different drivers

---

are biome-dependent, especially for land use change. It should be noted that effects of land use change on  $r_{veg}$  are mainly through changing  $k_w$ , with the largest value in croplands (+87%) and the smallest in boreal forests (-2%).

#### *4.3 Changes of soil carbon residence time*

Changes in decomposition and transfer rates among the soil carbon pools mainly explained the reduction of  $r_{soil}$ . Changes in climate mainly affected soil carbon decomposition rates (Bond-Lamberty, Bailey, Chen, Gough, & Vargas, 2018), and higher soil temperature and moisture are expected to accelerate soil organic carbon decomposition (Davidson & Janssens, 2006). At global scale, we find that CO<sub>2</sub> increase indirectly increased soil moisture, and had non-significant effects on soil temperature in the model simulation (Fig. S22). These combined effects increased the decomposition rates of soil organic carbon, that is, accelerated  $r_{soil}$ . This conclusion is line with experimental findings (Van Groenigen, Qi, Osenberg, Luo, & Hungate, 2014). In addition, climate change and land use change both increased global soil temperature and soil moisture (Fig. S22). The significant changes in the transfer rate between soil pools by the environmental changes may also contribute to the accelerated  $r_{soil}$ . For different biomes, the decomposition and transfer rates varied in magnitude in responses to environmental forcing (Fig. S22). Furthermore, land use change had the largest effect on the decomposition and transfer rates in cropland regions (Fig. S22), which is consistent with previous conclusions from field work using radiocarbon observations (Sanderman, Creamer, Baisden, Farrell, & Fallon, 2017).

#### *4.4 Ecosystem carbon storage potential*

Based on the model simulations of ecosystem states in the 2000s, our results indicate that tropical forests, especially in Amazon basin, will not provide such a strong carbon sink in the future, as they did in historical period. In addition, there is still a large carbon sink potential in terrestrial ecosystems, mostly in high northern latitudes, especially in the soil system. However, because of relatively slower soil decomposition and transformation rates in these cold regions (He et al., 2016), it requires thousands of years to accomplish this goal. It should be noted that, in reality, the ecosystem carbon potential is also changing based on given ecosystem states under

---

external forcing (e.g. atmospheric CO<sub>2</sub> concentration, climate and land cover types). Therefore, the ecosystem carbon potential evaluated in this way provides meaningfully theoretical estimates for the policy makers in a long-term perspective, and shows that the ecosystem carbon storage potential could be increased via sustainable means. For example, forest conservation and afforestation could improve the ecosystem carbon storage potential, by lengthening  $\tau_{eco}$  and increasing ecosystem productivity.

#### *4.5 Limitations of model*

In this study, the ORCHIDEE-MICT ecosystem model provided reasonable patterns of  $\tau_{eco}$  changes and their corresponding drivers, consistent with observation-based studies. Even so, the model still showed some major limitations which might obscure our understanding of the role of certain processes. First, in the experimental simulations, the dynamic global vegetation model (DGVM) module was not activated. Thus, the forest mortality rates were fixed for each plant functional type. This simplification may underestimate the magnitude of  $r_{veg}$  changes because forest mortality rates have been increasing universally in response to ongoing climate change (Allen et al., 2010; Brienen et al., 2015). The mechanisms of forest mortality include a series of physiological processes (e.g. carbon starvation and hydraulic failure) and external forces (e.g. windthrow, insect outbreaks, drought, competition and burning) associated with rising temperature and vapor pressure deficit (Choat et al., 2018; McDowell et al., 2018; Raffa et al., 2008; Stephenson et al., 2011). These effects are not fully incorporated in any DGVM. Introducing these complex processes in a DGVM model is challenging because we lack enough understanding of the operating rules of the vegetation turnover especially at the global scale. Due to the imperative of more comprehensive mortality schemes in DGVM models rather than fixed mortality rates, future DGVM modelers could probably sort out the major influential turnover-related drivers in corresponding regions rather than considering the all-side turnover-related processes in each region. For example, frost damage effects should be considered in boreal forests, and insect outbreaks should be considered in temperate forests (Thurner et al., 2016). Second, ORCHIDEE-MICT ecosystem model includes a structural improvement of soil carbon cycle

---

processes by discretizing the integral soil profile into multi layers including burial in permafrost (cryoturbation) and bioturbation. In a previous model evaluation (Guimberteau et al., 2018), it was showed that ORCHIDEE-MICT could capture the mean value and average vertical profile of soil organic carbon density in high-latitude regions. Another study by Huang et al. using a matrix-based representation of ORCHIDEE-MICT SOC also evaluated systematically the sensitive parameters among 34 parameters that control SOC profiles and found critical sensitivities to the active layer thickness and the cryoturbation rate (Huang et al., 2018). Here, to further improve the robustness of soil carbon turnover processes, we recommend that future versions should consider the radiocarbon data, which provide an independent constrain for the total soil carbon turnover (He et al., 2016; Lawrence et al., 2019; Mathieu, Hatté, Balesdent, & Parent, 2015; Trumbore, Sierra, & Hicks Pries, 2016). Third, nitrogen cycle plays an important role in regulating  $\tau_{eco}$ . For example, nitrogen availability could affect  $r_{veg}$  via changing carbon allocation (Friedlingstein, Joel, Field, & Fung, 1999; Li et al., 2020). In addition, nitrogen availability usually plays an impact on  $r_{soil}$  by altering the microbial activities and soil decomposition rates (Greaver et al., 2016; Janssens et al., 2010). The increase in nitrogen deposition (Galloway et al., 2004), could, therefore, affect changes in  $\tau_{eco}$ . Unfortunately, these effects cannot be evaluated in our study because ORCHIDEE-MICT did not include a coupled nitrogen cycle module.

We concluded that  $\tau_{eco}$  has generally accelerated between 1860s and 2000s. The mechanisms behind this acceleration vary across biomes and spatial scales, and the partitioning between  $r_{veg}$  and  $r_{soil}$  indicated different driving processes. Our study attributed the accelerating  $\tau_{eco}$  in a large degree to human-induced global change, with land use change playing a dominant role in most parts of the globe. Our analysis of the ecosystem carbon sink potential also show potential benefits of human actions by slowing  $\tau_{eco}$  by sustainable pathways, e.g. through land management, supporting their key role in keeping carbon for longer times in ecosystems.

### Acknowledgements

This study was supported by the National Key R&D Program of China (2017YFA0604702).

---

**Conflict of interest**

The authors declare that they have no conflict of interest.

**Data availability Statement**

All data used in this study are available from the corresponding author upon requests.

---

## References

- Allen, C. D., Macalady, A. K., Chenchouni, H., Bachelet, D., McDowell, N., Vennetier, M., . . . Cobb, N. (2010). A global overview of drought and heat-induced tree mortality reveals emerging climate change risks for forests. *Forest Ecology and Management*, 259(4), 660-684. <https://doi.org/10.1016/j.foreco.2009.09.001>
- Anderson, D. H. (1983). *Compartmental modeling and tracer kinetics*: Springer-Verlag.
- Arneth, A., Sitch, S., Pongratz, J., Stocker, B. D., Ciais, P., Poulter, B., . . . Zaehle, S. (2017). Historical carbon dioxide emissions caused by land-use changes are possibly larger than assumed. *Nature Geoscience*, 10(2), 79-84. <https://doi.org/10.1038/ngeo2882>
- Bolin, B. (1981). Steady state and response characteristics of a simple model of the carbon cycle. In *Carbon cycle modelling* (pp. 315-331): John Wiley and Sons, Somerset, NJ.
- Bond-Lamberty, B., Bailey, V. L., Chen, M., Gough, C. M., & Vargas, R. (2018). Globally rising soil heterotrophic respiration over recent decades. *Nature*, 560(7716), 80-83. <https://doi.org/10.1038/s41586-018-0358-x>
- Brienen, R. J., Phillips, O., Feldpausch, T., Gloor, E., Baker, T., Lloyd, J., . . . Lewis, S. (2015). Long-term decline of the Amazon carbon sink. *Nature*, 519(7543), 344-348. <https://doi.org/10.1038/nature14283>
- Bugmann, H., & Bigler, C. J. O. (2011). Will the CO<sub>2</sub> fertilization effect in forests be offset by reduced tree longevity? *Oecologia*, 165(2), 533-544. <https://doi.org/10.1007/s00442-010-1837-4>
- Carvalhais, N., Forkel, M., Khomik, M., Bellarby, J., Jung, M., Migliavacca, M., . . . Thurner, M. (2014). Global covariation of carbon turnover times with climate in terrestrial ecosystems. *Nature*, 514(7521), 213-217. <https://doi.org/10.1038/nature13731>
- Chen, C., Park, T., Wang, X., Piao, S., Xu, B., Chaturvedi, R. K., . . . Myneni, R. B. (2019). China and India lead in greening of the world through land-use management. *Nature Sustainability*, 2(2), 122-129. <https://doi.org/10.1038/s41893-019-0220-7>
- Choat, B., Brodribb, T. J., Brodersen, C. R., Duursma, R. A., López, R., & Medlyn, B. E. (2018). Triggers of tree mortality under drought. *Nature*, 558(7711), 531-539.

---

<https://doi.org/10.1038/s41586-018-0240-x>

- Ciais, P., Sabine, C., Bala, G., Bopp, L., Brovkin, V., Canadell, J., . . . Heimann, M. (2014). Carbon and other biogeochemical cycles. In *Climate change 2013: the physical science basis. Contribution of Working Group I to the Fifth Assessment Report of the Intergovernmental Panel on Climate Change* (pp. 465-570): Cambridge University Press.
- Davidson, E. A., & Janssens, I. A. (2006). Temperature sensitivity of soil carbon decomposition and feedbacks to climate change. *Nature*, 440(7081), 165-173.  
<https://doi.org/10.1038/nature04514>
- De Kauwe, M. G., Medlyn, B. E., Zaehle, S., Walker, A. P., Dietze, M. C., Wang, Y. P., . . . Hickler, T. (2014). Where does the carbon go? A model-data intercomparison of vegetation carbon allocation and turnover processes at two temperate forest free-air CO<sub>2</sub> enrichment sites. *New Phytologist*, 203(3), 883-899. <https://doi.org/10.1111/nph.12847>
- Erb, K.-H., Fetz, T., Plutzar, C., Kastner, T., Lauk, C., Mayer, A., . . . Haberl, H. (2016). Biomass turnover time in terrestrial ecosystems halved by land use. *Nature Geoscience*, 9(9), 674-678. <https://doi.org/10.1038/ngeo2782>
- Fernández-Martínez, M., Sardans, J., Chevallier, F., Ciais, P., Obersteiner, M., Vicca, S., . . . Peñuelas, J. (2019). Global trends in carbon sinks and their relationships with CO<sub>2</sub> and temperature. *Nature Climate Change*, 9(1), 73-79.  
<https://doi.org/10.1038/s41558-018-0367-7>
- Foley, J. A., DeFries, R., Asner, G. P., Barford, C., Bonan, G., Carpenter, S. R., . . . Snyder, P. K. (2005). Global consequences of land use. *Science*, 309(5734), 570-574.  
<https://doi.org/10.1126/science.1111772>
- Friedlingstein, P., Joel, G., Field, C. B., & Fung, I. Y. (1999). Toward an allocation scheme for global terrestrial carbon models. *Global Change Biology*, 5(7), 755-770.  
<https://doi.org/10.1046/j.1365-2486.1999.00269.x>
- Galloway, J. N., Dentener, F. J., Capone, D. G., Boyer, E. W., Howarth, R. W., Seitzinger, S. P., . . . Vöosmarty, C. J. (2004). Nitrogen Cycles: Past, Present, and Future. *Biogeochemistry*, 70(2), 153-226. <https://doi.org/10.1007/s10533-004-0370-0>

- Giglio, L., Randerson, J. T., & Werf, G. R. (2013). Analysis of daily, monthly, and annual burned area using the fourth-generation global fire emissions database (GFED4). *Journal of Geophysical Research: Biogeosciences*, 118(1), 317-328. <https://doi.org/10.1002/jgrg.20042>
- Goldewijk, K. K. (2001). Estimating global land use change over the past 300 years: The HYDE Database. *Global Biogeochemical Cycles*, 15(2), 417-433. <https://doi.org/10.1029/1999GB001232>
- Greaver, T. L., Clark, C. M., Compton, J. E., Vallano, D., Talhelm, A. F., Weaver, C. P., . . . Haeuber, R. A. (2016). Key ecological responses to nitrogen are altered by climate change. *Nature Climate Change*, 6(9), 836-843. <https://doi.org/10.1038/nclimate3088>
- Guimberteau, M., Zhu, D., Maignan, F., Huang, Y., Yue, C., Dantec-Nédélec, S., . . . Laurent, P. (2018). ORCHIDEE-MICT (v8. 4.1), a land surface model for the high latitudes: model description and validation. *Geoscientific Model Development*, 11, 121-163. <https://doi.org/10.5194/gmd-11-121-2018>
- He, Y., Trumbore, S. E., Torn, M. S., Harden, J. W., Vaughn, L. J. S., Allison, S. D., & Randerson, J. T. (2016). Radiocarbon constraints imply reduced carbon uptake by soils during the 21st century. *Science*, 353(6306), 1419-1424. <https://doi.org/10.1126/science.aad4273>
- Huang, Y., Zhu, D., Ciais, P., Guenet, B., Huang, Y., Goll, D. S., . . . Luo, Y. (2018). Matrix-based sensitivity assessment of soil organic carbon storage: A case study from the ORCHIDEE-MICT model. *Journal of Advances in Modeling Earth Systems*, 10(8), 1790-1808. <https://doi.org/10.1029/2017MS001237>
- Janssens, I., Dieleman, W., Luyssaert, S., Subke, J.-A., Reichstein, M., Ceulemans, R., . . . Matteucci, G. (2010). Reduction of forest soil respiration in response to nitrogen deposition. *Nature Geoscience*, 3(5), 315-322. <https://doi.org/10.1038/ngeo844>
- Joos, F., & Spahni, R. (2008). Rates of change in natural and anthropogenic radiative forcing over the past 20,000 years. *Proceedings of the National Academy of Sciences*, 105(5), 1425-1430. <https://doi.org/10.1073/pnas.0707386105>

- Knorr, W., Arneth, A., & Jiang, L. (2016). Demographic controls of future global fire risk. *Nature Clim. Change*, 6(8), 781-785. <https://doi.org/10.1038/nclimate2999>
- Kolby Smith, W., Reed, S. C., Cleveland, C. C., Ballantyne, A. P., Anderegg, W. R. L., Wieder, W. R., . . . Running, S. W. (2016). Large divergence of satellite and Earth system model estimates of global terrestrial CO<sub>2</sub> fertilization. *Nature Climate Change*, 6(3), 306-310. <https://doi.org/10.1038/nclimate2879>
- Koven, C., Chambers, J., Georgiou, K., Knox, R., Negron-Juarez, R., Riley, W., . . . Jones, C. (2015). Controls on terrestrial carbon feedbacks by productivity vs. turnover in the CMIP5 Earth System Models. *Biogeosciences*, 12(17), 5211-5228. <https://doi.org/10.5194/bg-12-5211-2015>
- Krinner, G., Viovy, N., de Noblet-Ducoudré, N., Ogée, J., Polcher, J., Friedlingstein, P., . . . Prentice, I. C. (2005). A dynamic global vegetation model for studies of the coupled atmosphere-biosphere system. *Global Biogeochemical Cycles*, 19(1), 1-33. <https://doi.org/10.1029/2003GB002199>
- Lawrence, C. R., Beem-Miller, J., Hoyt, A. M., Monroe, G., Sierra, C. A., Stoner, S., . . . Wagai, R. (2019). An open source database for the synthesis of soil radiocarbon data: ISRaD version 1.0. *Earth Syst. Sci. Data Discuss.*, 2019, 1-37. <https://doi.org/10.3929/ethz-b-000385703>
- Li, W., Zhang, H., Huang, G., Liu, R., Wu, H., Zhao, C., & McDowell, N. G. (2020). Effects of nitrogen enrichment on tree carbon allocation: A global synthesis. *Global Ecology and Biogeography*, 29(3), 573-589. <https://doi.org/10.1111/geb.13042>
- Liu, Y.W., Piao, S.L., Gasser, T., Ciais, P., Yang, H., Wang, H., . . . Wang T. (2019). Field-experiment constraints on the enhancement of the terrestrial carbon sink by CO<sub>2</sub> fertilization. *Nature Geoscience*, 12(10), 809-814. <https://www.nature.com/articles/s41561-019-0436-1>
- Lu, X., Wang, Y. P., Luo, Y., & Jiang, L. (2018). Ecosystem carbon transit versus turnover times in response to climate warming and rising atmospheric CO<sub>2</sub> concentration. *Biogeosciences*, 15, 6559-6572. <https://doi.org/10.5194/bg-15-6559-2018>

- Luo, Y., Keenan, T. F., & Smith, M. (2015). Predictability of the terrestrial carbon cycle. *Global Change Biology*, 21(5), 1737-1751. <https://doi.org/10.1111/gcb.12766>
- Luo, Y., Shi, Z., Lu, X., Xia, J., Liang, J., Jiang, J., . . . Ahlström, A. (2017). Transient dynamics of terrestrial carbon storage: mathematical foundation and its applications. *Biogeosciences*, 14(1), 145-161. <https://doi.org/10.5194/bg-14-145-2017>
- Luyssaert, S., Ciais, P., Piao, S. L., Schulze, E. D., Jung, M., Zaehle, S., . . . members of the, C.-I. S. T. (2010). The European carbon balance. Part 3: forests. *Global Change Biology*, 16(5), 1429-1450. <https://doi.org/10.1111/j.1365-2486.2009.02056.x>
- Mathieu, J. A., Hatté, C., Balesdent, J., & Parent, É. (2015). Deep soil carbon dynamics are driven more by soil type than by climate: a worldwide meta-analysis of radiocarbon profiles. *Global Change Biology*, 21(11), 4278-4292. <https://doi.org/10.1111/gcb.13012>
- McDowell, N., Allen, C. D., Anderson-Teixeira, K., Brando, P., Brienen, R., Chambers, J., . . . Xu, X. (2018). Drivers and mechanisms of tree mortality in moist tropical forests. *New Phytologist*, 219(3), 851-869. <https://doi.org/10.1111/nph.15027>
- McGrath, M. J., Luyssaert, S., Meyfroidt, P., Kaplan, J. O., Bürgi, M., Chen, Y., . . . Valade, A. (2015). Reconstructing European forest management from 1600 to 2010. *Biogeosciences*, 12(14), 4291-4316. <https://doi.org/10.5194/bg-12-4291-2015>
- Mouillot, F., & Field, C. B. (2005). Fire history and the global carbon budget: a  $1^\circ \times 1^\circ$  fire history reconstruction for the 20th century. *11(3)*, 398-420. <https://doi.org/10.1111/j.1365-2486.2005.00920.x>
- Pan, Y., Birdsey, R. A., Fang, J., Houghton, R., Kauppi, P. E., Kurz, W. A., . . . Canadell, J. G. (2011). A large and persistent carbon sink in the world's forests. *Science*, 333(6045), 988-993. <https://doi.org/10.1126/science.1201609>
- Peñuelas, J., Ciais, P., Canadell, J. G., Janssens, I. A., Fernández-Martínez, M., Carnicer, J., . . . Sardans, J. (2017). Shifting from a fertilization-dominated to a warming-dominated period. *Nature Ecology & Evolution*, 1(10), 1438-1445. <https://doi.org/10.1038/s41559-017-0274-8>
- Piao, S.L., Huang, M.T., Liu, Z., Wang, X.H., Ciais, P., Canadell, J.G., . . . Wang, T. (2018).

- Lower land use emissions responsible for increased net land carbon sink during the slow warming period. *Nature Geoscience*, 11(10), 739-743. <https://www.nature.com/articles/s41561-018-0204-7>
- Piao, S.L., Wang, X.H., Park, T.J., Chen, C., Lian, X., He, Y., . . . Myneni, R.B. (2020). Characteristics, driers and feedback of global greening. *Nature Reviews Earth & Environment*, 1(1), 14-27. <https://www.nature.com/articles/s43017-019-0001-x>
- Raffa, K. F., Aukema, B. H., Bentz, B. J., Carroll, A. L., Hicke, J. A., Turner, M. G., & Romme, W. H. (2008). Cross-scale drivers of natural disturbances prone to anthropogenic amplification: the dynamics of bark beetle eruptions. *BioScience*, 58(6), 501-517. <https://doi.org/10.1641/B580607>
- Ramankutty, N., & Foley, J. A. (1999). Estimating historical changes in global land cover: Croplands from 1700 to 1992. *Global Biogeochemical Cycles*, 13(4), 997-1027. <https://doi.org/10.1029/1999GB900046>
- Rasmussen, M., Hastings, A., Smith, M. J., Agusto, F. B., Chen-Charpentier, B. M., Hoffman, F. M., . . . Luo, Y. (2016). Transit times and mean ages for nonautonomous and autonomous compartmental systems. *Journal of Mathematical Biology*, 73(6), 1379-1398. <https://doi.org/10.1007/s00285-016-0990-8>
- Sanderman, J., Creamer, C., Baisden, W. T., Farrell, M., & Fallon, S. (2017). Greater soil carbon stocks and faster turnover rates with increasing agricultural productivity. *SOIL*, 3(1), 1-16. <https://doi.org/10.5194/soil-3-1-2017>
- Sierra, C. A., Ceballos-Núñez, V., Metzler, H., & Müller, M. (2018). Representing and understanding the carbon cycle using the theory of compartmental dynamical systems. *Journal of Advances in Modeling Earth Systems*, 10(8), 1729-1734. <https://doi.org/10.1029/2018MS001360>
- Sitch, S., Friedlingstein, P., Gruber, N., Jones, S., Murray-Tortarolo, G., Ahlström, A., . . . Huntingford, C. (2015). Recent trends and drivers of regional sources and sinks of carbon dioxide. *Biogeosciences*, 12(3), 653-679. <https://doi.org/10.5194/bg-12-653-2015>
- Stephenson, N. L., Van Mantgem, P. J., Bunn, A. G., Bruner, H., Harmon, M. E., O'Connell, K.

- B., . . . Franklin, J. F. (2011). Causes and implications of the correlation between forest productivity and tree mortality rates. *Ecological Monographs*, 81(4), 527-555. <https://doi.org/10.1890/10-1077.1>
- Thurner, M., Beer, C., Carvalhais, N., Forkel, M., Santoro, M., Tum, M., & Schmullius, C. (2016). Large-scale variation in boreal and temperate forest carbon turnover rate related to climate. *Geophysical Research Letters*, 43(9), 4576-4585. <https://doi.org/10.1002/2016GL068794>
- Trumbore, S. E., Sierra, C. A., & Hicks Pries, C. E. (2016). Radiocarbon nomenclature, theory, models, and interpretation: measuring age, determining cycling rates, and tracing source pools. In *Radiocarbon and climate change: mechanisms, applications and laboratory techniques* (pp. 45-82): Springer International Publishing.
- Van Groenigen, K. J., Osenberg, C. W., & Hungate, B. A. (2011). Increased soil emissions of potent greenhouse gases under increased atmospheric CO<sub>2</sub>. *Nature*, 475(7355), 214-216. <https://doi.org/10.1038/nature10176>
- Van Groenigen, K. J., Qi, X., Osenberg, C. W., Luo, Y., & Hungate, B. A. (2014). Faster decomposition under increased atmospheric CO<sub>2</sub> limits soil carbon storage. *Science*, 344(6183), 508-509. <https://doi.org/10.1126/science.1249534>
- Wei, Y., Liu, S., Huntzinger, D. N., Michalak, A., Viovy, N., Post, W., . . . Lu, C. (2014). The North American carbon program multi-scale synthesis and terrestrial model intercomparison project-Part 2: environmental driver data. *Geoscientific Model Development*, 7(6), 2875-2893. <https://doi.org/10.5194/gmd-7-2875-2014>
- Xia, J., Luo, Y., Wang, Y. P., & Hararuk, O. (2013). Traceable components of terrestrial carbon storage capacity in biogeochemical models. *Global Change Biology*, 19(7), 2104-2116. <https://doi.org/10.1111/gcb.12172>
- Yue, C., Ciais, P., Luyssaert, S., Li, W., McGrath, M. J., Chang, J., & Peng, S. (2018). Representing anthropogenic gross land use change, wood harvest, and forest age dynamics in a global vegetation model ORCHIDEE-MICT v8.4.2. *Geosci. Model Dev.*, 11(1), 409-428. <https://doi.org/10.5194/gmd-11-409-2018>
- Zhou, S., Liang, J., Lu, X., Li, Q., Jiang, L., Zhang, Y., . . . Luo, Y. (2018). Sources of uncertainty

---

in modeled land carbon storage within and across three MIPs: Diagnosis with three new techniques. *Journal of Climate*, 31(7), 2833-2851.  
<https://doi.org/10.1175/JCLI-D-17-0357.1>

Zhu, D., Peng, S., Ciais, P., Zech, R., Krinner, G., Zimov, S., & Grosse, G. (2016). Simulating soil organic carbon in yedoma deposits during the Last Glacial Maximum in a land surface model. *Geophysical Research Letters*, 43(10), 5133-5142.  
<https://doi.org/10.1002/2016GL068874>

Zhu, Z.C., Piao, S.L., Myneni, R.B., Huang, M.T., Zeng, Z.Z., Canadell, J.G., . . . Zeng, N. (2016). Greening of the earth and its drivers. *Nature Climate Change*, 6(8), 791-795.  
<https://www.nature.com/articles/nclimate3004>

---

## Figure legends:

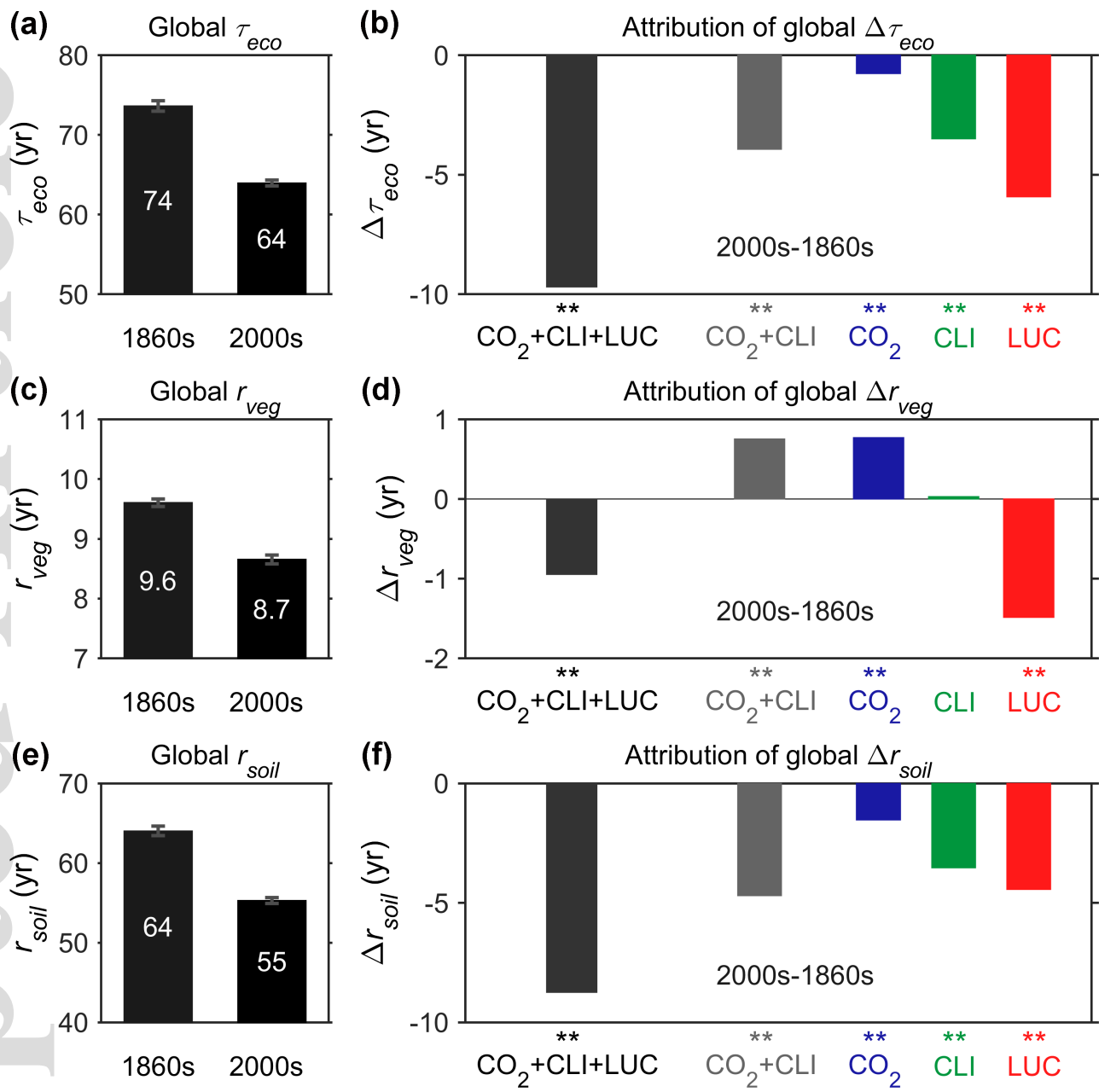
**Figure 1.** Global ecosystem carbon turnover time ( $\tau_{eco}$ ) in the 1860s and the 2000s (a) and attribution of their changes to driving factors (b). Driving factors include CO<sub>2</sub> increase (CO<sub>2</sub>), climate change (CLI) and land use change (LUC). Furthermore,  $\tau_{eco}$  is divided into carbon residence time in vegetation ( $r_{veg}$ ) and in soil ( $r_{soil}$ , including litter pools). The absolute values in the 1860s and the 2000s as well as their driving factors are shown in (c)-(d) for  $r_{veg}$  and in (e)-(f) for  $r_{soil}$ . Asterisks indicate significant differences ( $p < 0.05$ ) between the 1860s and the 2000s for  $\tau_{veg}$ ,  $r_{veg}$  or  $r_{soil}$ .

**Figure 2.** Ecosystem carbon turnover time ( $\tau_{eco}$ ) in the 1860s and the 2000s per biome. Biomes include boreal forest (BOF), temperate forest (TEF), tropical forest (TRF), grassland (GRA) and cropland (CRO). Furthermore,  $\tau_{eco}$  is divided into carbon residence time in vegetation ( $r_{veg}$ ) and in soil ( $r_{soil}$ , including litter pools). For each biome, absolute values of  $\tau_{eco}$ ,  $r_{veg}$  and  $r_{soil}$  in the 1860s and the 2000s are showed from left to right. Up-arrows (or down-arrows) represent significant ( $p < 0.05$ ) increase (or decrease) between the 1860s and the 2000s for  $\tau_{eco}$ ,  $r_{veg}$  or  $r_{soil}$ , accompanied with its dominant driving factor (CO<sub>2</sub> increase (CO<sub>2</sub>), climate change (CLI) or land use change (LUC)).

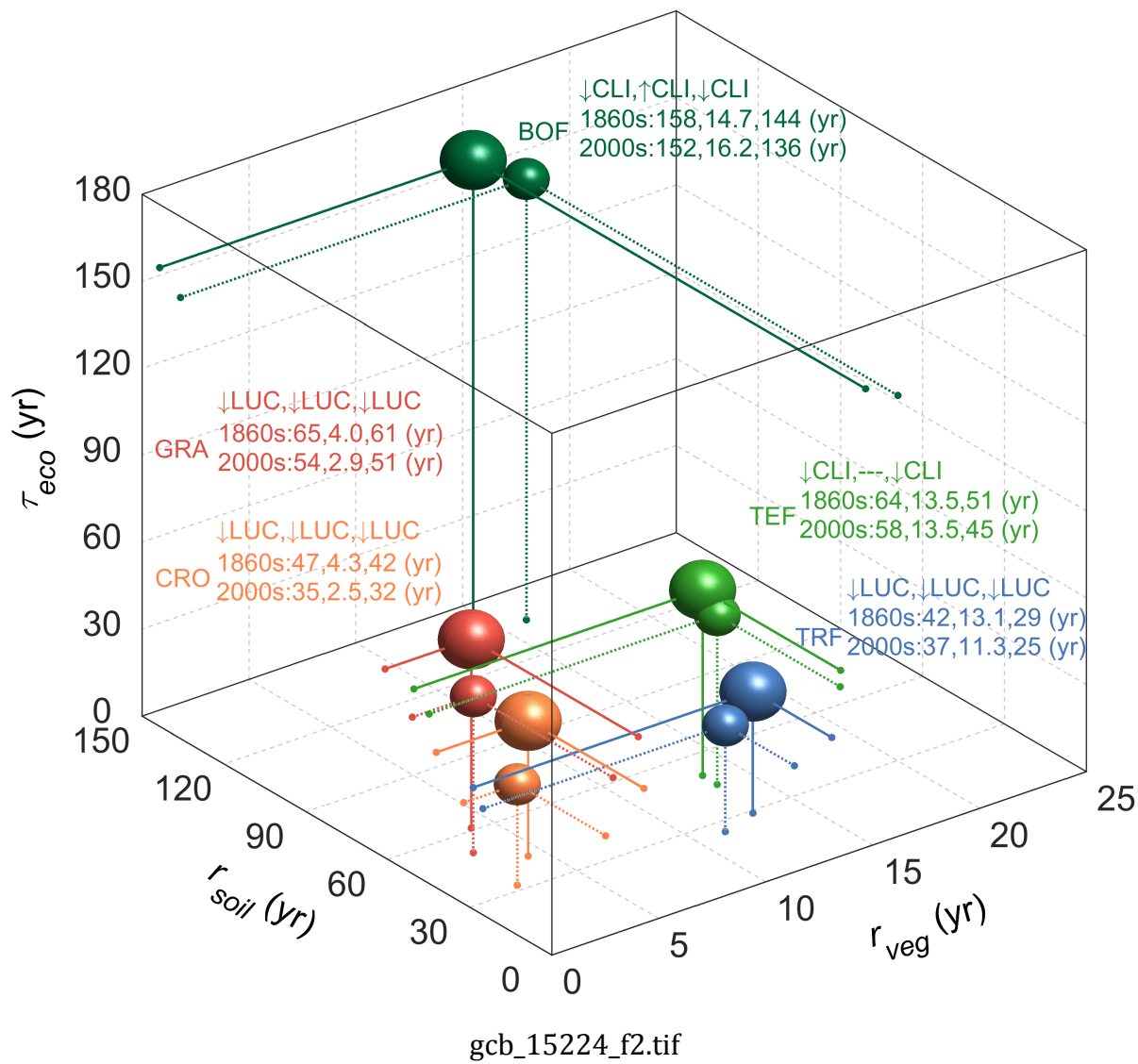
**Figure 3.** Ratio of ecosystem carbon turnover time ( $\tau_{eco}$ ) between the 2000s and the 1860s (a), and the corresponding dominant diving factor (b). Furthermore,  $\tau_{eco}$  is divided into carbon residence time in vegetation ( $r_{veg}$ ) and in soil ( $r_{soil}$ , including litter pools). Their ratio values between the 2000s and 1860s and dominant diving factor are shown in (c)-(d) for  $r_{veg}$  and in (e)-(f) for  $r_{soil}$ . In (a), (c) and (e), stippling indicates pixels with significant difference ( $p < 0.05$ ) between the 2000s and the 1860s for  $\tau_{eco}$ ,  $r_{veg}$  or  $r_{soil}$ . In (b), (d) and (f), driving factors include CO<sub>2</sub> increase (CO<sub>2</sub>), climate change (CLI) and land use change (LUC). A prefix '+' of the driving factors indicates a positive effect (slow-down) on  $\tau_{eco}$ ,  $r_{veg}$  or  $r_{soil}$ , whereas '-' indicates a negative effect (acceleration).

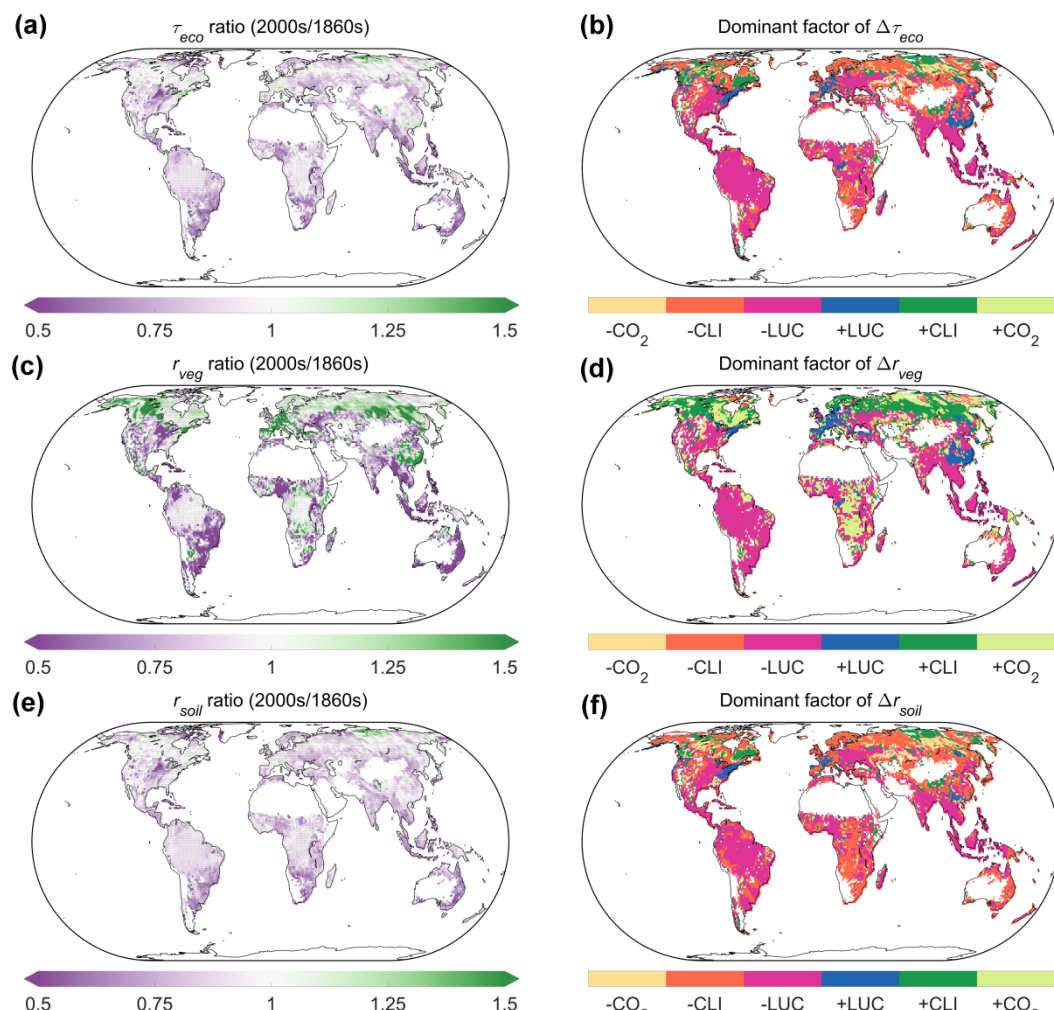
**Figure 4.** Spatial patterns of ecosystem carbon storage (Ceco) change between the 1860s and the

2000s (a), and ecosystem carbon storage potential based ecosystem state in the 2000s (b). Furthermore, ecosystem carbon storage is divided into vegetation carbon storage (Cveg) and soil carbon storage (Csoil, including litter carbon). Their corresponding carbon storage change between the 1860s and the 2000s and the carbon storage potential based ecosystem status in the 2000s are showed in (c)-(d) for Cveg and in (e)-(f) for Csoil. The right panel for each subgraph represents carbon storage changes or carbon storage potential averaged by latitude.

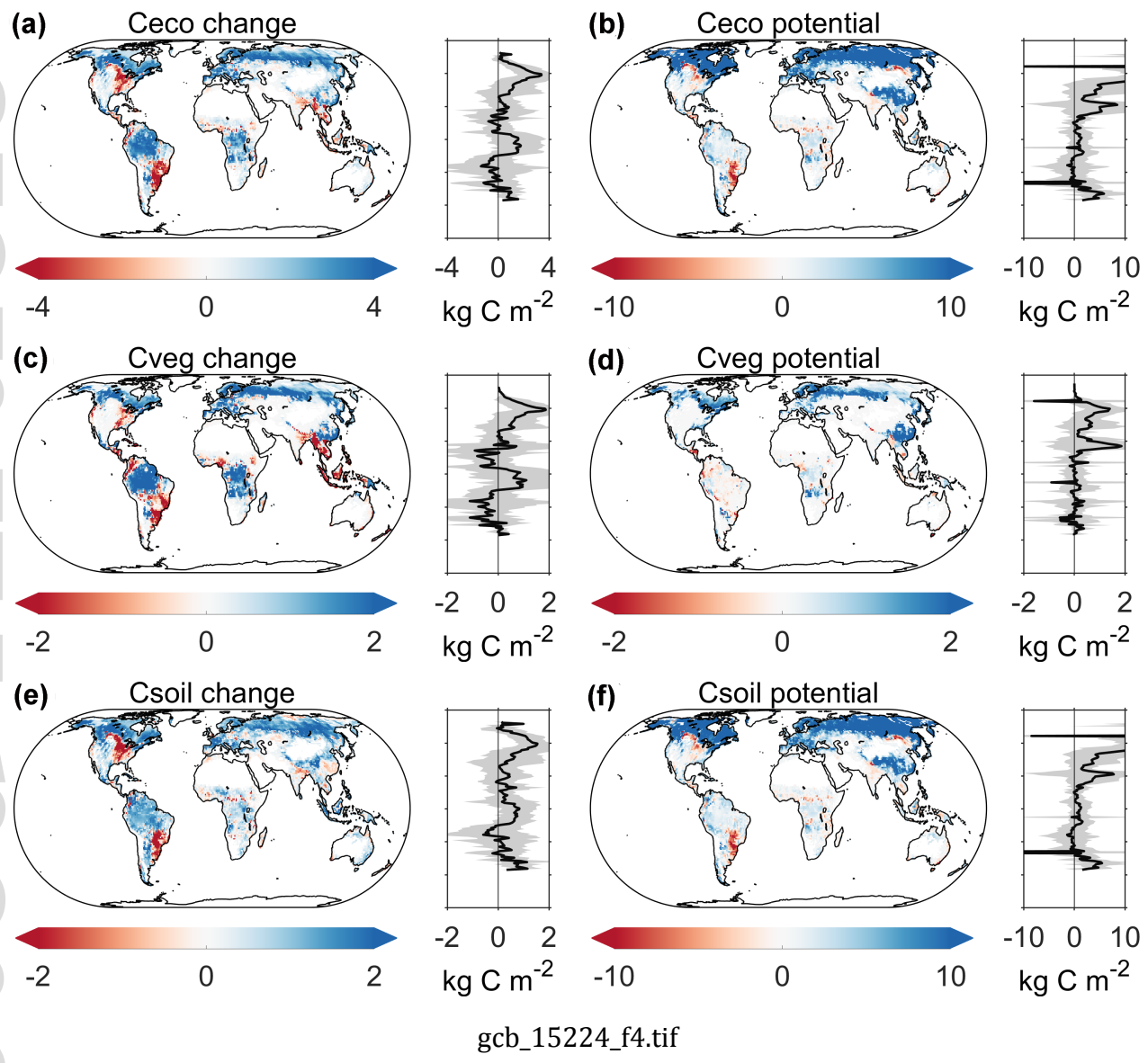


gcb\_15224\_f1.tif





gcb\_15224\_f3.tif



gcb\_15224\_f4.tif